



# *eIF6* Promotes Gastric Cancer Proliferation and Invasion by Regulating Cell Cycle

Cong-Gai Huang<sup>1,2</sup> · Xiao-Qing Zhou<sup>1</sup> · An-Fu Zheng<sup>3</sup> · Xing Luo<sup>1</sup> · Jing Shen<sup>3</sup> · Zhan-Gang Xiao<sup>3</sup> · Zhi-Hui Yang<sup>1,2</sup> · Qiong Dai<sup>4</sup>

Received: 21 March 2024 / Accepted: 23 April 2024 / Published online: 10 July 2024  
© The Author(s) 2024

## Abstract

**Objective** To investigate the role and function of *eIF6* in gastric cancer (GC).

**Methods** The expression level of *eIF6* in GC tissues and normal tissues was detected in different high-throughput sequencing cohorts. Survival analysis, gene differential analysis, and enrichment analysis were performed in the TCGA cohort. Biological networks centered on *eIF6* were constructed through two different databases. Immunohistochemistry (IHC) and Western blot were used to detect protein expression of *eIF6*, and qRT-PCR was used to detect *eIF6* mRNA expression. The correlation between the expression of *eIF6* in GC tissues and clinicopathological parameters of GC was analyzed. siRNA knockout of *eIF6* was used to study the proliferation, migration, and invasion. The effects of *eIF6* on cell cycle and Cyclin B1 were detected by flow cytometry and Western blot.

**Results** *eIF6* was significantly overexpressed in GC tissues and predicted poor prognosis. In addition, 113 differentially expressed genes were detected in cancer-related biological pathways and functions by differential analysis. Biological networks revealed interactions of genes and proteins with *eIF6*. The expression intensity of *eIF6* in cancer tissues was higher than that in adjacent tissues ( $P=0.0001$ ), confirming the up-regulation of *eIF6* expression in GC tissues. The expression level of *eIF6* was statistically significant with pTNM stage ( $P=0.006$ ). siRNA knockout of *eIF6* significantly reduced the proliferation, colony formation, migration, and invasion ability of GC cells. Silencing of *eIF6* also inhibited the cell cycle of GC cells in G2/M phase and decreased the expression level of CyclinB1.

**Conclusion** Our study suggests that *eIF6* is up-regulated in GC and may promote the proliferation, migration, and invasion of GC by regulating cell cycle.

**Keywords** Eukaryotic translation factor 6 · Gastric cancer · Cell cycle · CyclinB1

## Introduction

According to the latest data on the global cancers burden, gastric cancer (GC) ranks fifth in incidence and fourth in mortality [1]. The incidence of GC shows significant regional differences, with West Asian countries having the highest incidence. At present, the incidence rate of GC in East Asia is on the rise. A series of molecular and genetic changes have been found in GC, including multiple oncogenes, tumor suppressor genes, and signal pathways related genes [2]. Individualized treatment of GC requires early and accurate diagnosis [3]. In China, more than 80% of patients are not diagnosed until the advanced stage of GC, so many patients miss the opportunity of radical resection or face the high risk of postoperative metastasis and recurrence [4]. Therefore, the pathogenesis of GC needs to be further

✉ Qiong Dai  
daiqiong@swmu.edu.cn

Zhi-Hui Yang  
yzhih73@swmu.edu.cn

<sup>1</sup> Department of Pathology, The Affiliated Hospital of Southwest Medical University, Luzhou 646000, Sichuan, People's Republic of China

<sup>2</sup> Precision Pathology Diagnosis for Serious Diseases Key Laboratory of LuZhou, Luzhou, People's Republic of China

<sup>3</sup> Department of Pharmacy, Southwest Medical University, Luzhou, People's Republic of China

<sup>4</sup> Department of Human Anatomy, Southwest Medical University, Luzhou 646000, Sichuan, People's Republic of China

explored, which may help to early diagnosis, prognostic evaluation, and treatment decisions.

Protein translation includes a series of processes, including initiation, extension, termination, and circulation [5]. Eukaryotic translation initiation factors (eIFs) play an important regulatory role in the initiation phase of translation. The eIFs family includes *eIF1*, *eIF2*, *eIF3*, *eIF4*, *eIF5*, and *eIF6* [6]. *eIF6* is the speed limiting factor in the last step of initiation, which can effectively avoid the premature binding of 60S subunit and 40S subunit, and play a unique anti-binding role [7–9]. *eIF6* participates in the composition of multiple protein complexes related to RNA-induced silencing complex (RISC) and plays a key role in the regulation of miRNA activity. Study has shown that the deletion of *eIF6* in human cell lines can lead to the inhibition of miRNA activity [10].

*eIF6* is abnormally expressed in a variety of malignant tumors, with high expression in head and neck squamous cell carcinoma (HNSCC) [11], non-small cell lung cancer (NSCLC) [12], breast cancer [13], hepatocellular carcinoma (HCC) [14], gallbladder cancer (GBC) [7], colorectal cancer (CRC) [15], malignant mesothelioma (MM) [16], ovarian serous adenocarcinoma [17], and pancreatic cancer [18]. However, the role of *eIF6* in GC has not been studied. To explore the role and function of *eIF6* in the carcinogenesis of GC, the expression levels of *eIF6* in GC tissues and normal tissues were detected in different high-throughput sequencing cohorts. Survival analysis, differential analysis, and enrichment analysis were performed in the TCGA cohort. Biological networks centered on *eIF6* were constructed through two different databases. We also used immunohistochemistry (IHC) to detect the relative expression of *eIF6* in GC and adjacent tissues, and then used siRNA to establish GC cell line, and detected the effect of silencing *eIF6* on its proliferation, migration, invasion, and cycle to provide a new theoretical basis for the progression of GC.

## Materials and Methods

### Bioinformatics Analysis

The bulk RNA-seq data and survival data of GC were downloaded from TCGA database: TCGA-STAD. Groups were constructed based on the expression levels of *eIF6*, and differentially expressed genes were identified by the R package limma. KEGG enrichment analysis and GO enrichment analysis of differentially expressed genes were performed using R package ClusterProfiler and Using the Hiplot portal (<https://hiplot.com.cn>) to visualize the enrichment analysis results. The STRING database (<https://string-db.org>) enabled the identification of proteins promising interactions with *eIF6* and the construction of PPI. The PPI was further

embellished using Cytoscape. The GENEMANIA (<http://www.genemania.org>) is a database used to construct biological networks for gene prioritization and predict gene function. Here we identified genes with a potential shared function with *eIF6* through GENEMANIA.

### Cell Lines and Culture

Human GC cell line HGC27 was purchased from Shanghai Cell Bank, Chinese Academy of Sciences, and four other GC cell lines SGC7901, AGS, MGC803, BGC823 were donated by the department of Pathology of the Southern Medical University. The three small interfering RNA fragments (siRNA-1, siRNA-2, siRNA-3) and negative control interfering RNA fragments (siRNA-NC) of *eIF6* were designed and synthesized by Guangzhou Ruibo Biotechnology. All the cells used in the experiment were adherent cells, which were cultured with RPMI 1640 medium (placed in 5% CO<sub>2</sub> atmosphere incubator and at 37 °C), and the cells used in the experiment grew well.

### Tissue Microarray

Human GC tissue chip was purchased from Shanghai Xinchao Biotechnology Co., LTD (Catalog number: HStmA180Su08-M-047). In the tissue microarray, 100 GC tissues were used as study group and 80 normal adjacent tissues (NATs) were used as control group (5 cm away from the lesion). This study was approved by the Medical Ethics Committee of the First Affiliated Hospital of Southwest Medical University (KY2022274).

### Immunohistochemistry

The GC tissue microarray was baked in a 60 °C constant temperature oven overnight. The tissue microarray was immersed in EDTA repair solution (pH 8.0). 3% formaldehyde H<sub>2</sub>O<sub>2</sub> solution was uniformly dripped onto the tissue. 5% goat serum was evenly dripped onto the tissue and closed at 37 °C for 30 min in wet box. The monoclonal rabbit anti-*eIF6* (Catalog number: #3263S; 1:100 dilution; Cell Signaling Technology) was incubated at 4 °C overnight in wet box. On the second day, after incubation, secondary antibody kit (Catalog number: #ZLI-9032, Zhongshan Jinqiao Biotechnology) was used and incubated at 37 °C for 30 min in wet box. After adding an appropriate amount of DAB color developing solution, observe the color development under the microscope in time. All IHC results were independently interpreted by two pathologists and scored according to the staining intensity and positive proportion of tumor cells [19]. According to the positive proportion of tumor cells, no positive cells were scored 0 points, positive cells no more than 10% were rated 1 point, positive cells accounted for 1%

to 49% of tumor cells were rated 2 points, positive cells accounted for 50% to 79% were rated 3 points, positive cells accounted for 80% to 100% were rated 4 points. According to the cell coloring depth score, no coloring was scored 0 points, light brown yellow was scored 1 point, brown yellow was scored 2 points, brown was scored 3 points. Multiply the scores of the above two indicators, a score of 0 was interpreted as negative, a score of 1 to 4 was interpreted as weak positive, a score of 5 to 8 was interpreted as moderate positive, and a score of 9 to 12 was interpreted as strong positive.

### Lentivirus Infection

The sequences of siRNAs were as follows: siRNA-1 (CAT GCGGGATCCCTCATT), siRNA-2 (ATCGGAGGCTCA GAGAACT), siRNA-3 (GAGTGTCTTCAAGCTGAAT). GC cells ( $2 \times 10^5$  cells/well) were seeded in six-well plate with Opti-MEM culture medium (1990  $\mu$ L), siRNA storage solution (5  $\mu$ L), and of Lipofectamine 2000 transfection reagent (5  $\mu$ L) at 5% CO<sub>2</sub> and 37 °C. After 24 h of transfection, the expression level of *eIF6* mRNA was detected by real-time quantitative PCR (qRT-PCR). Western blot was used to detect the expression of *eIF6* protein of transfection 48 h.

### RNA Isolation and qRT-PCR

PCR assay total RNA was isolated from GC cells using Trizol (Takara). A total of 500 ng RNA was reversely transcribed into complementary DNA (cDNA) with High-Capacity cDNA Reverse Transcription Kits (Takara), followed by qRT-PCR detection by SYBR® Premix Ex Taq mix (TaKaRa). The qRT-PCR primers involved were designed and chemo-synthesized by Shanghai Shenggong Bioengineering, *eIF6* F: 5'-CCGCGTGCGGAGCTTGTT A-3'; R: 5'-CGCCCTCGAACACACTGTAGAAGT-3';  $\beta$ -actin F: 5'-GCTCGTCGTCGACAACGGCTC-3'; R: 5'-ATCTTCAAACCTCCATGATG-3'. Relative mRNA expression was normalized to  $\beta$ -actin using  $2^{-\Delta\Delta CT}$  method. The annealing temperature was set at 60 °C.

### Western Blot

GC cells were lysed by RIPA Lysis Buffer (Beyotime), protein was extracted and its concentration was determined (Solarbio). The membrane was blocked with 5% skimmed milk for 1 h after protein electrophoresis and membrane transfer. After cleaning the membranes with TBST, membranes were incubated with primary antibodies CyclinB1 (Catalog number: #12231S, 1:1,000; Cell Signaling Technology), *eIF6* (Catalog number: #3263S, 1:1,000; Cell Signaling Technology), and  $\beta$ -actin (Catalog number: BS6007MH, 1:2000; Bioworld) at 4 °C overnight. Blots were performed with a peroxidase-conjugated fluorescent

secondary antibody for 1 h, and then the western blots were scanned and semi-quantitatively analyzed on a Vision Works chemiluminescence imager and uses corresponding software to process stripes.

### CCK-8 Assay

GC cells ( $5 \times 10^3$  cells/well) were cultured in a 96-well plate containing RPMI-1640 medium. The cells were then cultured for 24 h, 48 h, 72 h, and 96 h, with 10  $\mu$ L CCK-8 reagent (Beyotime, China) added to each well and cultured for another 2 h. Optical density values were evaluated at 450 nm using a microplate reader (BMG Labtech, USA) and statistical line plots were made.

### Plate Cloning Test

The GC cells after 48 h of transfection were selected, washed, and digested into cell suspension, and then counted. Add the prepared high serum medium to adjust the cell concentration. The cells were inoculated with 500 cells/well in a 6-well culture plate (determined according to cell growth and pre-experimental results). Each group had three multiple wells and 2 mL medium per well. The cells were continued to be cultured for 7–14 days. After the plate cloning test, the cells were washed twice with PBS, fixed with 1 mL 4% paraformaldehyde per well for 30–60 min, 1 mL crystal violet dye solution per well for about 30 min. The cells were counted manually by taking pictures with a digital camera (the whole six-well plate and each well were taken separately and clearly). Clone-forming rate = (number of clones/numbers of inoculated cells)  $\times$  100%.

### Wound-Healing Assay

Inoculate GC cells on a 6-well plate, with  $3 \times 10^5$  cells in each well. Draw straight lines on the bottom of the 6-well plate with a 10  $\mu$ L needle (each group is set with three replicates, and each group repeats the experiment three times). Under the inverted phase contrast microscope, observe the width of the scratch in the same field at 0 h, 24 h, and 48 h ( $\times$  100), take photos and record, and use image J software to analyze and record the scratch image.

### Transwell Assay

100  $\mu$ L serum-free medium containing  $2 \times 10^4$  cells were added to the Transwell chamber, 1640 medium containing 10%FBS was added to the lower chamber, and then placed in cell incubator at 37 °C for 48 h (repeated three times for each group). Transwell assay was terminated and the results were further evaluated. The process of cell fixation and staining in the chamber was the same as that of plate cloning test.

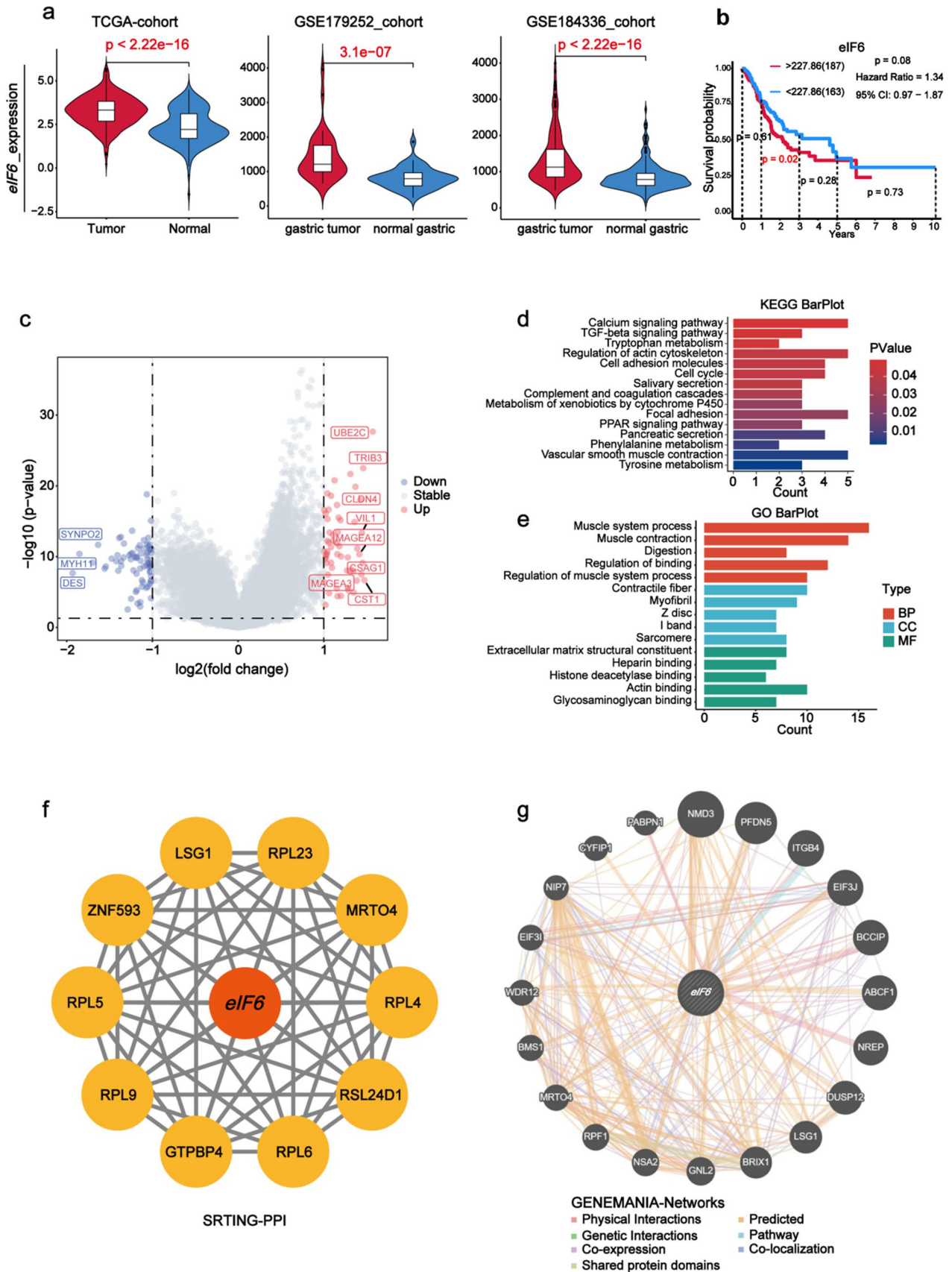


**Fig. 1** Bioinformatics landscape of *eIF6* in gastric cancer. **a** Violin plots for comparison of *eIF6* expression levels between tumor tissues and normal tissues in different high-throughput sequencing cohorts. **b** Survival curves of gastric cancer samples in the TCGA cohort grouped based on *eIF6* expression levels. **c** Volcano plot for differential analysis performed with grouping by *eIF6* expression levels. **d**, **e** Bar plot of partial results of KEGG and GO enrichment analysis of differentially expressed genes. **f** Protein–protein interaction network constructed by STRING database. **g** Gene network with shared biological functions centered on *eIF6* constructed by GENEMANIA database

Under the microscope, the remaining cells that did not pass through the polycarbonate membrane were gently swabbed with a cotton swab and the invading cells were counted in five random areas. The number of cells invaded was counted using the Image J software.

### Flow Cytometry

Cells stimulated by siRNA-*eIF6* for 48 h were collected with good growth and cell density of about 50–70%, and each group was set with 3 wells. Resuspended cells were digested with pancreatin without EDTA and precipitates were collected. Gently blow to make a single cell suspension, and fix it in a refrigerator at 4 °C overnight. Take out the fixed cells, gently blow them into a single cell suspension with 1 mL precooled PBS, and transfer them into 1.5 mL EP tube. Add 500 µL PI/RNase staining buffer, incubate in dark for 30 min, detect the cell cycle distribution with flow cytometry within 1 h, record and analyze the results.

### Statistical Analysis

The GraphPad Prism 8 software was used for statistical analysis of the experimental data. The expression of *eIF6* protein in GC and adjacent tissues and the relationship between the expression level of *eIF6* and clinicopathological parameters of patients were analyzed by chi-square test or Fisher exact probability method to compare the rates between groups. The results of CCK8 experiment were analyzed by one-way ANOVA, and the *t* test was used to compare two independent samples in other experiments. All Bioinformatics statistical analyses were performed using R software (v4.2.0). Wilcoxon test and Kruskal–Wallis's test were used for comparison of *eIF6* expression levels between different clinical parameter groupings. Kaplan–Meier curves with the log-rank test were performed for survival analysis.  $P < 0.05$  indicates that the difference is statistically significant.

## Results

### *eIF6* Is Dysregulated in Gastric Cancer with Prognostic Potential

In the TCGA cohort of gastric cancer, *eIF6* expression level was significantly higher in tumor tissues than in normal tissues ( $P < 0.05$ ). Survival analysis showed that there was no significant difference in overall survival (OS) between high *eIF6* expression group and low *eIF6* expression group ( $P > 0.05$ ). Since there was no statistical difference in the results of survival analysis based on the TCGA cohort, and we found that there were intersecting segments in the survival curve, we further divided the survival time into intervals and conducted survival analysis separately. The results showed that patients with high *eIF6* expression had a significantly lower overall survival rate than patients with low *eIF6* expression in the range of 1 to 3 years of survival, so *eIF6* has a potential cancer-promoting effect (Fig. 1a, 1b).

### Functional Enrichment Analysis and Potential Regulatory Network of *eIF6* in Gastric Cancer

A total of 75 significantly down-regulated genes and 58 significantly up-regulated genes were obtained ( $|\log\text{FC}| > 1$ ,  $P < 0.05$ ). KEGG enrichment analysis showed that differentially expressed genes were significantly enriched in cell cycle pathways. In GO enrichment analysis, differentially expressed genes were significantly enriched in both biological processes and cellular components related to the muscle system. In addition, differentially expressed genes were significantly enriched in extracellular matrix, heparin binding, and other molecular functions. To further analyze the downstream regulatory network of *eIF6*, we constructed a protein–protein interaction network centered on *eIF6* through the STRING database. Consistently, the components in the protein–protein interaction network were significantly associated with ribosome-related biological functions. In addition, we constructed an *eIF6*-centered regulatory network from seven aspects using the GENEMANIA database. These genes may potentially share biological functions with *eIF6* (Fig. 1).

### *eIF6* Is Up-Regulated in GC Tissues

Of 100 cases of GC tissues detected by IHC, the results showed that *eIF6* expression was negative in 7 cases (7.0%), weakly positive in 35 cases (35.0%), moderately positive in 31 cases (31.0%), and strongly positive in 26 cases (27.0%). Of the 80 cases of NATs, 11 were negative (13.8%), 49 were weakly positive (61.3%), 20 were moderately positive

(25.0%), and 0 were strongly positive (0.0%). There was a statistically significant difference in the expression of *eIF6* between GC tissues and NATs ( $\chi^2 = 19.710$ ,  $P = 0.0001$ ) (Table 1), and the expression of *eIF6* was significantly up-regulated in GC tissues. *eIF6* yellow–brown particles are mainly located in the cytoplasm, as shown in Fig. 2a.

### Expression Level of *eIF6* Has Statistical Significance with pTNM Stage of GC

The relationship between clinicopathological characteristics and the expression of *eIF6* showed that *eIF6* was only statistically correlated with pTNM stage ( $P < 0.05$ ), but not with age, sex, degree of differentiation, lymph node metastasis, and distant metastasis ( $P > 0.05$ ) (Table 1).

### AGS and MGC803 with High Expression of *eIF6* in GC Cell Line

The level of *eIF6* mRNA and protein expression in GC cell lines HGC27, SGC7901, AGS, MGC803, and BGC823 were

detected by qRT-PCR and Western blot. The results showed that the level of *eIF6* mRNA in AGS and MGC803 cells was high (Fig. 2b), and the level of protein expression in AGS, MGC803, and BGC823 cell lines was high (Fig. 2c). The cell lines AGS and MGC803 with high mRNA and protein expression were selected for subsequent experiments.

### *eIF6* Promotes Proliferation, Migration, and Invasion of GC Cells In Vitro

The interference efficiency of three siRNA fragments was detected by qRT-PCR and Western blot (Fig. 2d, e). siRNA-2 and siRNA-3 were used to interfere with the *eIF6* of cells in subsequent experiments. The changes in the proliferative capacity of AGS/MGC803 cell line after siRNA silencing *eIF6* were measured by CCK8. The results showed that the OD value of AGS/MGC803 cell line in the experimental group silencing *eIF6* was significantly lower than that in the negative control (NC) group at different time points, and the difference was statistically significant ( $P < 0.05$ ) (Fig. 3a). Plate cloning test showed that the ability of colony-forming

**Table 1** The relationship between *eIF6* expression and clinicopathological characteristics

Characteristics	N	<i>eIF6</i> expression		$\chi^2$	P
		Negative and weak	Moderately and strongly		
<i>Type</i>				19.710	0.0001
GC	100	42(42.0%)	58(58.0%)		
NAT	80	60(75.0%)	20(25.0%)		
<i>Age (year)</i>				1.236	0.266
< 60	32	16(50.0%)	16(50.0%)		
≥ 60	68	26(38.2%)	42(61.8%)		
<i>Gender</i>				0.138	0.710
Male	64	26(40.6%)	38(59.4%)		
Female	36	16(44.4%)	20(55.6%)		
<i>Tumor size</i>				0.001	0.980
< 5 cm	43	18(41.9%)	25(58.1%)		
≥ 5 cm	57	24(42.1%)	33(57.9%)		
<i>Differentiation degree</i>				3.435	0.185
Low	15	4(26.7%)	11(73.3%)		
Medium	74	31(41.9%)	43(58.1%)		
High	11	7(63.6%)	4(36.3%)		
<i>pTNM</i>				<b>7.532</b>	<b>0.006</b>
II + II-III	37	9(24.3%)	28(75.7%)		
III + III-IV	63	33 (52.4%)	30(47.6%)		
<i>Lymph node metastasis</i>				0.024	0.877
No	27	11(40.7%)	16(59.3%)		
Yes	73	31(42.5%)	42(57.6%)		
<i>Distant metastasis</i>				0.735	0.486
No	91	37(40.7%)	54(28.6%)		
Yes	9	5(55.6%)	4(44.4%)		

Bold values indicate that the pathological parameter difference was statistically significant

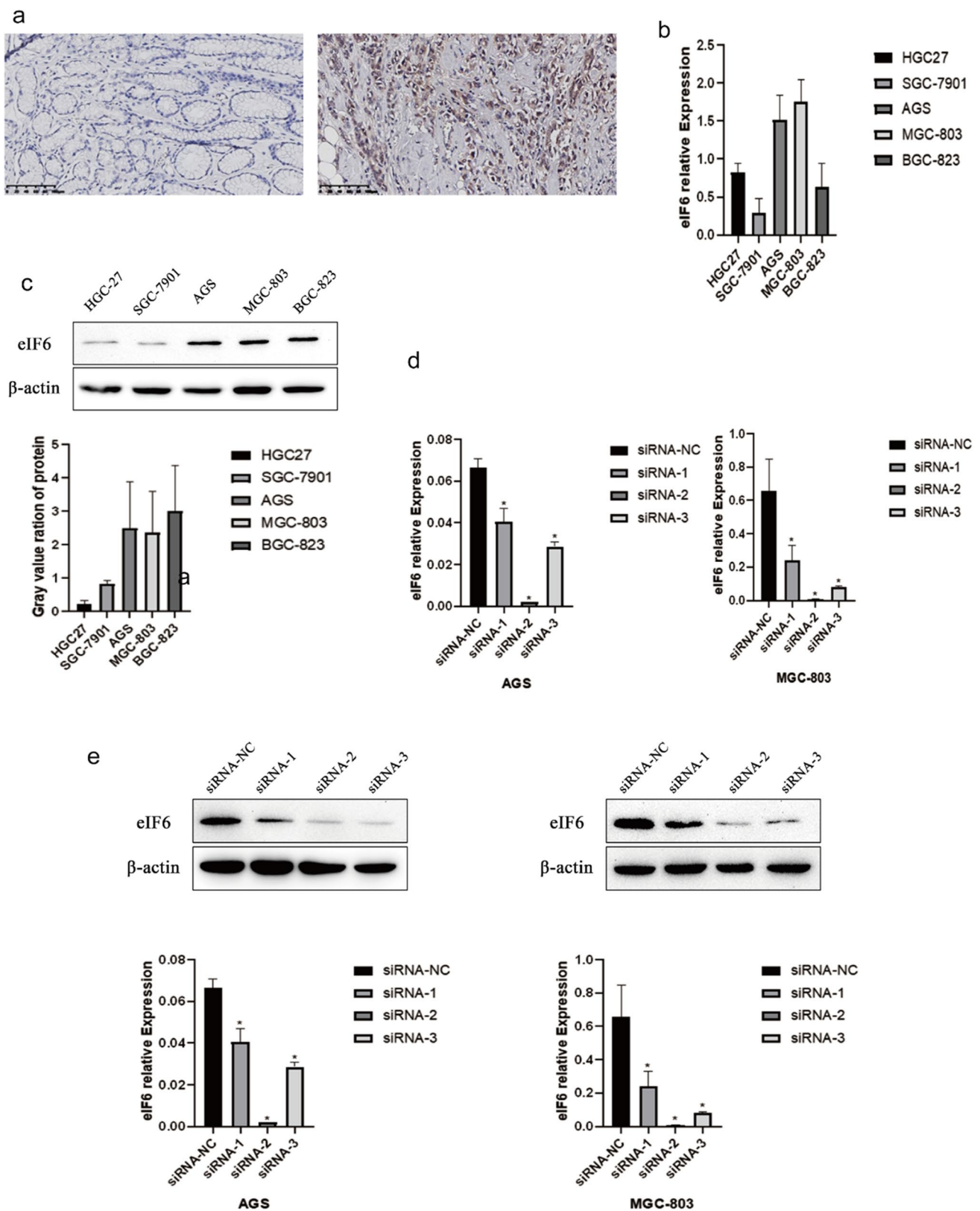


**Fig. 2** The expression of *eIF6* in GC tissues and cells. **A** IHC was used to detect the expression of *eIF6* in 80 normal adjacent tissues and 100 GC tissues ( $\times 200$ ). **b** qRT-PCR was used to detect the expression of *eIF6* in GC cells. **c** Western blot was used to detect

the expression of *eIF6* in GC cells. **d** Gray ratio histogram in AGC/MGC803 cell lines. **e** *eIF6* protein expression was detected by Western blot after siRNA interference (\*Compared with siRNA-NC group,  $P < 0.05$ )

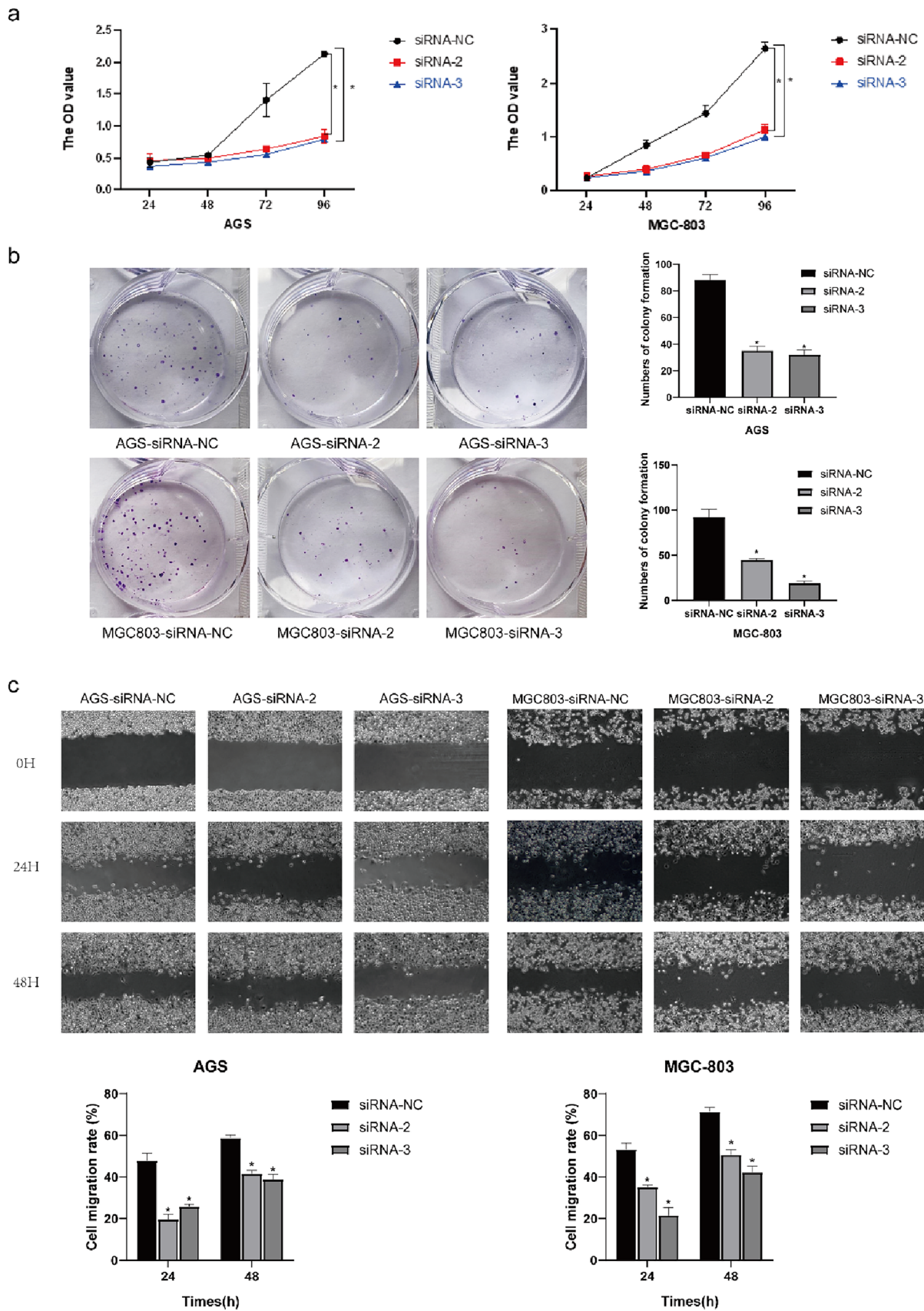




**Fig. 3** *eIF6* promotes proliferation and migration of GC cells in vitro. **a** CCK8 assays detected the proliferation of gastric cancer lines with silence of *eIF6* in vitro. **b** The effects of silent *eIF6* on colony formation abilities AGS/MGC803 cells in vitro. **c** Wound-healing assays detect the migration abilities of gastric cancer lines with silence of *eIF6* in vitro ( $\times 40$ ) (\*,  $P < 0.05$ )

of GC cells in vitro decreased after silencing *eIF6* (Fig. 3b). The wound-healing assay results showed that the migration ability of GC cells in vitro decreased after silencing *eIF6* (Fig. 3c). Similarly, the Transwell assays showed that the invasion ability of GC cells in vitro decreased after silencing *eIF6* (Fig. 4a).

### Silencing of *eIF6* in GC Cells Can Block Cell Cycle at G2/M Phase

Flow cytometry was used to detect the cell cycle of AGS/MGC803 cells after silencing of *eIF6* (Fig. 4b). The results showed that silencing of *eIF6* in GC cells blocked the G2/M phase. Meanwhile, Western blot results also showed reduced expression of cyclin B1 (Fig. 4c).

## Discussion

GC remains a high-risk malignancy, both for incidence and mortality. The treatment methods of GC include surgery, radiotherapy, chemotherapy, immunotherapy, and molecular targeted therapy. Although the treatment methods have been greatly improved, the prognosis of GC has not been substantially improved [20–22]. The occurrence of GC is influenced and involved by multiple factors, steps, and genes, which is a complex process. At present, research has found that it involves changes in molecular and genetic levels of multiple oncogenes, cell cycle regulatory, and DNA repair genes. The activation of oncogene is the driving factor of tumor, so targeted therapy has become a research hotspot in the treatment of GC [2, 23]. eIFs are involved in growth factors, cell cycle, translation of growth proteins, and cell apoptosis. *eIF6* is a rate-limiting factor in the process of cell cycle and tumorigenesis, plays a unique anti-binding role in the initiation of translation, and participates in the process of ribosome [10, 24].

Our research results indicated that *eIF6* was significantly up-regulated in GC patients and was associated with worsening prognosis (Fig. 1). At the clinical pathological tissue level, we further investigated and found that the expression of *eIF6* protein was significantly higher in GC tissues than in adjacent cancerous tissues (Fig. 2). As the key protein factor in the process of protein translation initiation, the eIFs play an important role in the control of protein translation that regulates cell growth, apoptosis, and malignant

transformation [25]. Related studies point to the identity of *eIF6* as a risk prognostic factor in HCC, CRC, NSCLC, and MM [12, 15, 26, 27]. The *eIF6* promoter contains GA-rich sequences in which the GABP complex has been identified as a regulator of *eIF6* express [28]. GABP is a widely studied transcription factor involved in the regulation of tumor proliferation, ribosome, and metabolism [29]. Our results suggest that silencing of *eIF6* can reduce the malignant biological behavior of GC cells, including cell proliferation, migration, and invasion (Figs. 3, 4). Hao et al. pointed out that the eIFs are aberrantly dysregulated in human cancers and can serve as potential therapeutic targets for cancer [30]. In a mouse model of lymphoma, impairment of cytoplasmic *eIF6* activity inhibited the development of lymphoma [9]. The function of the eIFs is mainly regulated by mammalian target of rapamycin (mTOR), and almost all signaling pathways are involved in mTOR signaling transduction [30]. mTOR is usually activated in cancer, controlling cell growth and metabolism [31]. In our study, enrichment analysis showed that differentially expressed downstream genes of *eIF6* were significantly enriched in pathways such as tyrosine metabolism (Fig. 1). It is noteworthy that the cell cycle and TGF-beta signaling pathways were significantly enriched. Signaling pathways that promote tumorigenesis have growth factor signaling transduction characteristics, which can strongly stimulate the activation of signaling pathways such as ERK, MAPK, and PI3K/AKT [32]. The activity of the cell cycle pathway is usually regulated by signaling pathways such as PI3K-AKT and MAPK [33, 34]. Therefore, we propose that due to the abnormal activation of signaling pathways such as PI3K-AKT and MAPK during GC progression, the mTOR signaling transduction is regulated, resulting in the abnormal dysregulation of *eIF6*. Then, the dysregulation of *eIF6* activates the cell cycle pathway, further promoting the differentiation of tumor cells, and ultimately leading to poor prognosis. Flow cytometry results showed that GC cell lines with silenced *eIF6* were arrested in the G2/M phase (Fig. 4). This further illustrates the critical role of *eIF6* in tumor progression. In addition, we constructed a protein–protein interaction (PPI) network centered on *eIF6* and a gene regulatory network for functional sharing (Fig. 1). We found that proteins interacting with *eIF6* were highly enriched in ribosome-related biological processes, which is related to the role of *eIF6* as the initiator factor of protein translation [35]. Interestingly, these interacting proteins were significantly associated with the biological function of ubiquitin ligase inhibitor activity. Ubiquitination modification regulates tumor suppression and promotion pathways, and targeting the ubiquitin system is a promising approach for the treatment of inflammatory diseases, cancer, and other diseases [36]. The link between *eIF6* and ubiquitination modification may be an innovative research direction.

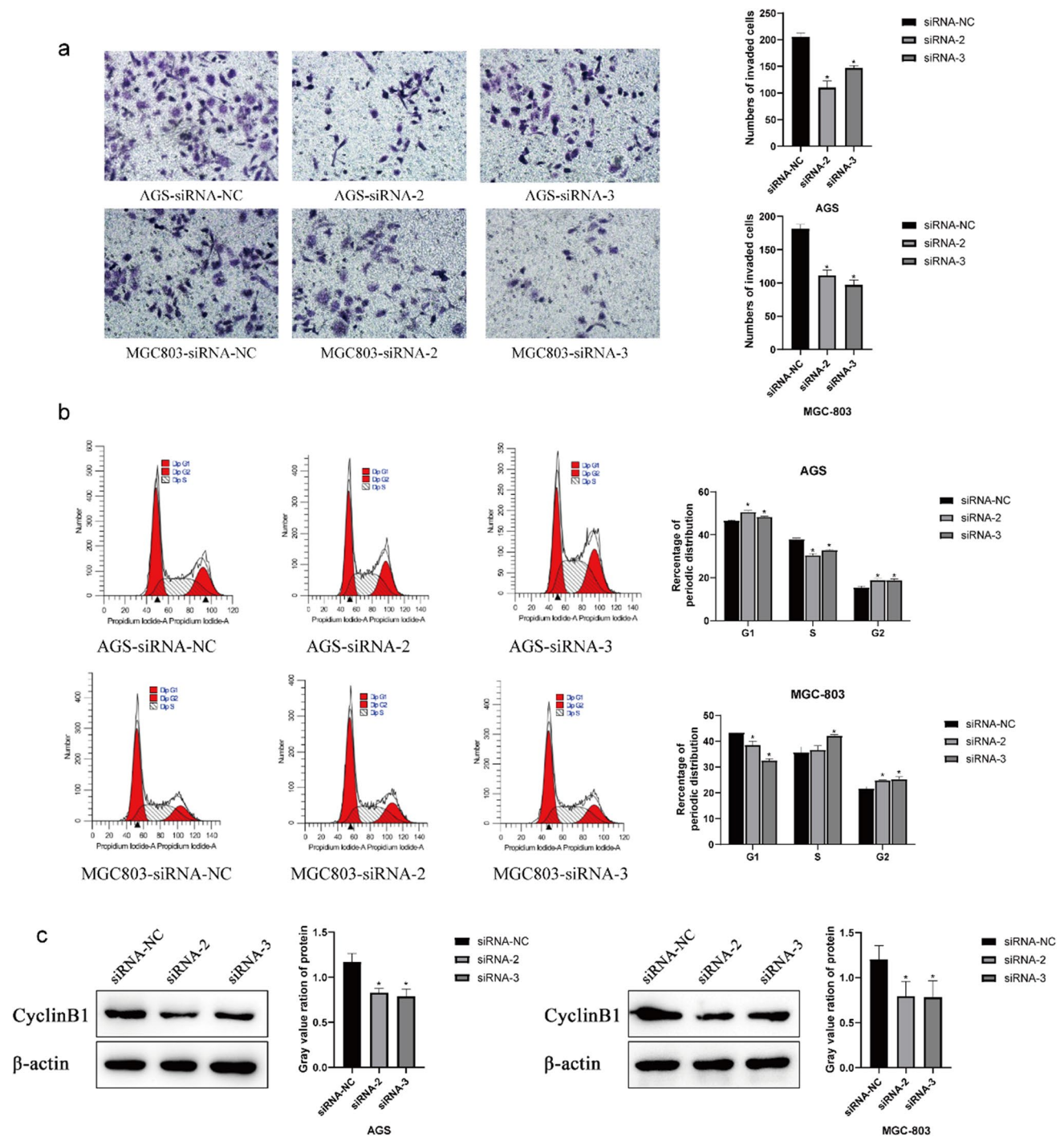


**Fig. 4** *eIF6* promotes invasion and changes cell cycle of GC cells in vitro. **a** Transwell assays detect the invasion abilities of gastric cancer lines with silence of *eIF6* in vitro ( $\times 100$ ). **b** Flow cytometry

detect the cell cycle of gastric cancer lines with silence of *eIF6* in vitro (\*,  $P < 0.05$ ). **c** Western blot detect the expression of CyclinB1 of gastric cancer lines with silence of *eIF6* (\*,  $P < 0.05$ )

In conclusion, our results show that the expression of *eIF6* protein in GC tissues is higher than that in adjacent tissues, and the expression of *eIF6* protein is related to the pTNM stage of tumors. In GC cell line, silencing of *eIF6* can inhibit cell proliferation, migration, and invasion

abilities and change the cell cycle. These results suggest that *eIF6* may promote the malignant biological behavior of GC by regulating the cell cycle. Subsequently, we will further study and elucidate the molecular mechanism of *eIF6* in GC.

**Acknowledgments** Thanks go to Johannes Haybaeck for providing excellent ideas and assistance.

**Author's contributions** HCG and ZXQ made major contributions to the data analysis and manuscript writing. ZAF collected the data and participated in writing the manuscript. LX, SJ and XZG participated in collecting data. DQ and YZH were participated in research designing and idea, writing and revising the manuscript. All authors discussed, carefully read and approved the final manuscript. All data generated or analyzed during this study are included in this article. Further enquiries can be directed to the corresponding author.

**Funding** This work was financially supported by Sichuan Science and Technology Program (No. 2022YFS0636) and Luzhou Science and Technology Program (No.2022-SYF-39).

## Declarations

**Conflict of interest** The authors declare that they have no competing interests.

**Ethical approval** This study was approved by the Medical Ethics Committee of the Affiliated Hospital of Southwest Medical University (KY2022274).

**Open Access** This article is licensed under a Creative Commons Attribution-NonCommercial 4.0 International License, which permits any non-commercial use, sharing, adaptation, distribution and reproduction in any medium or format, as long as you give appropriate credit to the original author(s) and the source, provide a link to the Creative Commons licence, and indicate if changes were made. The images or other third party material in this article are included in the article's Creative Commons licence, unless indicated otherwise in a credit line to the material. If material is not included in the article's Creative Commons licence and your intended use is not permitted by statutory regulation or exceeds the permitted use, you will need to obtain permission directly from the copyright holder. To view a copy of this licence, visit <http://creativecommons.org/licenses/by-nc/4.0/>.

## References

- Sung H, Ferlay J, Siegel RL et al. Global Cancer Statistics 2020: GLOBOCAN Estimates of Incidence and Mortality Worldwide for 36 Cancers in 185 Countries. *CA Cancer J Clin*. 2021;71:209–249.
- Molina-Castro S, Pereira-Marques J, Figueiredo C, Machado JC, Varon C. Gastric cancer: Basic aspects. *Helicobacter*. 2017;22:1.
- Wang FH, Zhang XT, Li YF et al. The Chinese Society of Clinical Oncology (CSCO): Clinical guidelines for the diagnosis and treatment of gastric cancer, 2021. *Cancer Commun (Lond)*. 2021;41:747–795.
- Yamamoto M, Rashid OM, Wong J. Surgical management of gastric cancer: The East vs. West perspective. *J Gastrointest Oncol*. 2015;6:79–88.
- Silvera D, Arju R, Darvishian F et al. Essential role for eIF4GI overexpression in the pathogenesis of inflammatory breast cancer. *Nat Cell Biol*. 2009;11:903–908.
- Spilka R, Ernst C, Mehta AK, Haybaeck J. Eukaryotic translation initiation factors in cancer development and progression. *Cancer Lett*. 2013;340:9–21.
- Golob-Schwarzl N, Wodlej C, Kleinegger F et al. Eukaryotic translation initiation factor 6 overexpression plays a major role in the translational control of gallbladder cancer. *J Cancer Res Clin Oncol*. 2019;145:2699–2711.
- Golob-Schwarzl N, Schweiger C, Koller C et al. Separation of low and high grade colon and rectum carcinoma by eukaryotic translation initiation factors 1, 5 and 6. *Oncotarget*. 2017;8:101224–101243.
- Miluzio A, Beugnet A, Grosso S et al. Impairment of cytoplasmic eIF6 activity restricts lymphomagenesis and tumor progression without affecting normal growth. *Cancer Cell*. 2011;19:765–775.
- Hock J, Weinmann L, Ender C et al. Proteomic and functional analysis of Argonaute-containing mRNA-protein complexes in human cells. *EMBO Rep*. 2007;8:1052–1060.
- Rosso P, Cortesina G, Sanvito F et al. Overexpression of p27BPP in head and neck carcinomas and their lymph node metastases. *Head Neck*. 2004;26:408–417.
- Gantenbein N, Bernhart E, Anders I et al. Influence of eukaryotic translation initiation factor 6 on non-small cell lung cancer development and progression. *Eur J Cancer*. 2018;101:165–180.
- Li Y, Wang Z, Su P et al. circ-EIF6 encodes EIF6-224aa to promote TNBC progression via stabilizing MYH9 and activating the Wnt/beta-catenin pathway. *Mol Ther*. 2022;30:415–430.
- Scagliola A, Miluzio A, Mori G, et al. Inhibition of eIF6 activity reduces hepatocellular carcinoma growth: An in vivo and in vitro study. *Int J Mol Sci*. 2022;23:720.
- Lin J, Yu X, Xie L et al. eIF6 Promotes Colorectal Cancer Proliferation and Invasion by Regulating AKT-Related Signaling Pathways. *J Biomed Nanotechnol*. 2019;15:1556–1567.
- Miluzio A, Oliveto S, Pesce E et al. Expression and activity of eIF6 trigger malignant pleural mesothelioma growth in vivo. *Oncotarget*. 2015;6:37471–37485.
- Zhu W, Li GX, Chen HL, Liu XY. The role of eukaryotic translation initiation factor 6 in tumors. *Oncol Lett*. 2017;14:3–9.
- Zhang T, Li M, Lu H, Peng T. Up-Regulation of circEIF6 Contributes to Pancreatic Cancer Development Through Targeting miR-557/SLC7A11/PI3K/AKT Signaling. *Cancer Manag Res*. 2021;13:247–258.
- Remmele W, Stegner HE. Recommendation for uniform definition of an immunoreactive score (IRS) for immunohistochemical estrogen receptor detection (ER-ICA) in breast cancer tissue. *Pathologe*. 1987;8:138–140.
- He W, Tu J, Huo Z et al. Surgical interventions for gastric cancer: a review of systematic reviews. *Int J Clin Exp Med*. 2015;8:13657–13669.
- Aoyama T, Yoshikawa T. Adjuvant therapy for locally advanced gastric cancer. *Surg Today*. 2017;47:1295–1302.
- Takei S, Kawazoe A, Shitara K. The new era of immunotherapy in gastric cancer. *Cancers (Basel)*. 2022;14:1054.
- Yang L, Gu HJ, Zhu HJ et al. Tissue inhibitor of metalloproteinase-2 G-418C polymorphism is associated with an increased risk of gastric cancer in a Chinese population. *Eur J Surg Oncol*. 2008;34:636–641.
- Miluzio A, Beugnet A, Volta V, Biffo S. Eukaryotic initiation factor 6 mediates a continuum between 60S ribosome biogenesis and translation. *EMBO Rep*. 2009;10:459–465.
- Robichaud N, Sonenberg N, Ruggiero D, Schneider RJ. Translational control in cancer. *Cold Spring Harb Perspect Biol*. 2019;11:a032896.
- Sun L, Liu S, Wang X, Zheng X, Chen Y, Shen H. eIF6 promotes the malignant progression of human hepatocellular carcinoma via the mTOR signaling pathway. *J Transl Med*. 2021;19:216.
- Zhang F, Waheed S, Armato U, Wu J, Zhang C, Li Z. eIF6 as a Promising Diagnostic and Prognostic Biomarker for Poorer Survival of Cutaneous Melanoma. *Front Oncol*. 2022;12:848346.
- Donadini A, Giacomelli F, Ravazzolo R, Gandin V, Marchisio PC, Biffo S. GABP complex regulates transcription of eIF6 (p27BPP),

- an essential trans-acting factor in ribosome biogenesis. *FEBS Lett.* 2006;580:1983–1987.
29. Rosmarin AG, Resendes KK, Yang Z, McMillan JN, Fleming SL. GA-binding protein transcription factor: a review of GABP as an integrator of intracellular signaling and protein-protein interactions. *Blood Cells Mol Dis.* 2004;32:143–154.
  30. Hao P, Yu J, Ward R et al. Eukaryotic translation initiation factors as promising targets in cancer therapy. *Cell Commun Signal.* 2020;18:175.
  31. Mossmann D, Park S, Hall MN. mTOR signalling and cellular metabolism are mutual determinants in cancer. *Nat Rev Cancer.* 2018;18:744–757.
  32. Silvera D, Formenti SC, Schneider RJ. Translational control in cancer. *Nat Rev Cancer.* 2010;10:254–266.
  33. Chang F, Lee JT, Navolanic PM et al. Involvement of PI3K/Akt pathway in cell cycle progression, apoptosis, and neoplastic transformation: a target for cancer chemotherapy. *Leukemia.* 2003;17:590–603.
  34. Margadant C, Cremers L, Sonnenberg A, Boonstra J. MAPK uncouples cell cycle progression from cell spreading and cytoskeletal organization in cycling cells. *Cell Mol Life Sci.* 2013;70:293–307.
  35. Zhang L, Zhang Y, Zhang S, et al. Translational Regulation by eIFs and RNA Modifications in Cancer. *Genes (Basel).* 2022;13:2050.
  36. Cockram PE, Kist M, Prakash S, Chen SH, Wertz IE, Vucic D. Ubiquitination in the regulation of inflammatory cell death and cancer. *Cell Death Differ.* 2021;28:591–605.

**Publisher's Note** Springer Nature remains neutral with regard to jurisdictional claims in published maps and institutional affiliations.